

UNCLASSIFIED

AD 419315

DEFENSE DOCUMENTATION CENTER

FOR

SCIENTIFIC AND TECHNICAL INFORMATION

CAMERON STATION, ALEXANDRIA, VIRGINIA



UNCLASSIFIED

NOTICE: When government or other drawings, specifications or other data are used for any purpose other than in connection with a definitely related government procurement operation, the U. S. Government thereby incurs no responsibility, nor any obligation whatsoever; and the fact that the Government may have formulated, furnished, or in any way supplied the said drawings, specifications, or other data is not to be regarded by implication or otherwise as in any manner licensing the holder or any other person or corporation, or conveying any rights or permission to manufacture, use or sell any patented invention that may in any way be related thereto.

ASD-TDR-63-647

CATALOGED BY JDC
AS AD No. 41 9315

419315

MATERIAL DAMPING UNDER BIAXIAL STATE OF STRESS GENERATED BY COMBINED AXIAL AND INTERNAL PRESSURE LOADINGS

64-5-

TECHNICAL DOCUMENTARY REPORT NO. ASD-TDR-63-647

JULY 1963

AF MATERIALS LABORATORY
AERONAUTICAL SYSTEMS DIVISION
AIR FORCE SYSTEMS COMMAND
WRIGHT-PATTERSON AIR FORCE BASE, OHIO

Project No. 7351, Task No. 735106

(Prepared under Contract No. AF 33(657)-7453
by the University of Minnesota, Minneapolis, Minn.
T. J. Mentel and S. H. Chi, authors)

NOTICES

When Government drawings, specifications, or other data are used for any purpose other than in connection with a definitely related Government procurement operation, the United States Government thereby incurs no responsibility nor any obligation whatsoever; and the fact that the Government may have formulated, furnished, or in any way supplied the said drawings, specifications, or other data, is not to be regarded by implication or otherwise as in any manner licensing the holder or any other person or corporation, or conveying any rights or permission to manufacture, use, or sell any patented invention that may in any way be related thereto.

Qualified requesters may obtain copies of this report from the Defense Documentation Center (DDC), (formerly ASTIA), Arlington Hall Station, Arlington 12, Virginia.

This report has been released to the Office of Technical Services, U.S. Department of Commerce, Washington 25, D.C., for sale to the general public.

Copies of this report should not be returned to the Aeronautical Systems Division unless return is required by security considerations, contractual obligations, or notice on a specific document.

FOREWORD

This report was prepared by the University of Minnesota, Department of Aeronautics and Engineering Mechanics under USAF Contract No. AF 33(657)-7453. This contract was initiated under Project No. 7351, "Metallic Materials," Task No. 735106, "Behavior of Metals." The work was administered under the direction of the AF Materials Laboratory, Aeronautical Systems Division. Mr. J. P. Henderson was the project engineer.

The experimental work described in this report was carried out in the period February 1962 to September 1962.

The authors would like to thank Dr. B. J. Lazan for his advice concerning the experimental set-up and Mr. David L. Beste for his assistance in the reduction of the experimental results. Manuscript typing was by Miss Nancy Ahlbrecht.

ABSTRACT

A test machine has been constructed which measures material damping in thin-walled, cylindrical specimens subject to combined internal pressure and axial cyclic loading. The purpose of this machine is to allow the complete range of biaxial stress states to be developed, so that the individual damping effects of distortional and dilatational straining action might be clearly discerned. Experimental results on a series of manganese alloy specimens are found to display significant damping effect associated with dilatational straining.

This technical documentary report has been reviewed and is approved.



W. J. TRAPP
Chief, Strength and Dynamics Branch
Metals and Ceramics Division
Air Force Materials Laboratory

TABLE OF CONTENTS

	PAGE
I. INTRODUCTION	1
II. TEST APPARATUS	2
III. CALIBRATION ACCURACY AND PRECISION OF APPARATUS	3
IV. SELECTION OF TEST MATERIAL	5
V. THEORETICAL CONSIDERATIONS WITH RESPECT TO DATA REDUCTION	6
VI. EXPERIMENTAL RESULTS	9
VII. DISCUSSION OF RESULTS AND CONCLUSIONS	10
VIII. REFERENCES	12

LIST OF FIGURES

FIGURE		PAGE
1	Schematic of Test Apparatus	13
	(Legend for Figure 1)	14
2	Overall Test Set-Up	15
3	Axial and Pressure Crank Geometries	16
4	Displacement Waveform Distortion	17
5	Strain Gage Disposition and Bridge Set-Ups . .	18
6	Geometry of Test Specimens	19
7	Comparison of Parameters for Depicting Energy Ratios	20
8	Basic Trend Curves for Material Damping . . .	21
9	Alternate Presentation of Trend Curves	21
10	Typical Hysteresis Loops for $a = 1/8$ and $a = -1/2$	22
11	Typical Phase-Check Loops Corresponding to Figure 11	23
12	Stress History Check with Uniaxial Stress . .	24
13	Stress History Check with Biaxial Stress . . .	24
14	Experimental Results, Specimen A	25
15	Experimental Results, Specimen A, Alternate Plot	26
16	Experimental Results, Specimen B	27
17	Experimental Results, Specimen C	28
18	Experimental Results, Specimen D	29
19	Experimental Results, Specimen E	30

I. INTRODUCTION

This paper describes an experimental study of cyclic material damping in thin-walled, cylindrical specimens of manganese copper alloy, subject to combined axial and internal pressure loading. The objective of this study is to determine precisely the importance of dilatational straining action in the production of material damping. Present experimental results of material damping, for structural metals under biaxial states of stress, indicate that only the distortional straining action is associated with detectable internal damping phenomena. This means that the specific damping of a structural metal, which we measure in inch pounds of energy dissipated per cubic inch of material per cycle of loading, can be correlated for different states of stress solely referring to the respective distortional straining amplitudes. This enables a simple similarity criterion to be written which identifies biaxial with uniaxial states of stress for a given material, which produce the same specific damping.

An important contribution to the study of material damping under biaxial states of stress was made by Robertson and Yorgiadis [1]*, who found that in order to produce the same specific damping, the amplitude of the shear stress in the biaxial stress case had to be between 0.48 and 0.60 of the amplitude of the normal stress in the uniaxial stress case. Their suggested value $1/\sqrt{3}$ implies that the expressions for the distortional strain energies, modified by the total neglect of the mean normal stress component, be equal in the two states. This introduces the notion of two-dimensional distortional and dilatational strain as identified by the maximum shear and mean normal stress components respectively. A symbolic statement of this similarity condition is

$$\sigma_n = \sqrt{3} \tau_n$$

where σ_n is the normal stress amplitude in the uniaxial state and τ_n is the maximum shear stress amplitude in the biaxial state.

The foregoing criterion has subsequently been confirmed by several experimenters, but only under certain broad limits of experimental scatter. Furthermore, the test conditions have always been such that the distortional straining action was the dominant deformation process. The typical experimental test set-up has employed either a bar or a tubular specimen subjected to combined axial and torsional loading.

* Numbers in parentheses refer to references on page 12 .
Manuscript released for publication April 1963 as an ASD
Technical Documentary Report.

It was conjectured by Mentel [2], that since in the case of plate vibrations, wherein dilatational straining generally accounts for a much larger share of the total straining action, it might also be found to be significant in material damping production. The implication of this conjecture is that the absence of damping effects due to dilatational straining observed of structural metals hitherto has been due to the restricted test set-ups and the masking effect of large experimental scatter.

The problem thus posed was the extension of the experimental test conditions to include those corresponding to plate vibrations. The first tests would be made with materials already well examined experimentally in the previous studies. If these proposed tests revealed a positive damping effect associated with dilatational straining, then a simple revision of the mathematical statement of the similarity condition for equal damping under uniaxial and biaxial stress states is [2]

$$\sigma_n = \sqrt{3 \tau_m^2 + \lambda \sigma_d^2} \quad (1)$$

where σ_d is the "mean normal" stress in the biaxial stress state. If the principal stresses are given by σ_1 and σ_2 , then

$$\sigma_1 = \sigma_d + \tau_m, \quad \sigma_2 = \sigma_d - \tau_m. \quad (2)$$

The value of $\lambda = 0$ produces the Robertson-Yorgiadis criterion, and $\lambda = 1$ produces the distortional strain energy criterion wherein the three-dimensional elasticity description of distortional and dilatational straining action is applied. The experimental study described herein produces a value of $\lambda = 1.2$ for a manganese copper alloy.

II. TEST APPARATUS

A schematic of the internal pressure and axial loading system is shown in Figure 1. The hollow, cylindrical, test specimen A is joined to a similarly constructed axial load transducer B which employs electric strain gages about its circumference. The lower end of the test specimen is attached to a sliding rod C which in turn is attached by flexplate D to the lever E. The lever E is hinged by a flexural pivot F and driven at the other hand by the crank G. The crank is powered by an electric motor with variable speed control H. The usual speed of testing was from 1 to 5

cycles per second.

The pressure loading system is driven synchronously from G by the second crank mechanism J. The stepped hydraulic jack K acts as a cyclic pressure inducing device and is fitted with a spring L to prevent the load component arising from high mean pressure from being transmitted back through the pulley system G-J. The cyclic variation in the fluid pressure directly stresses specimen and the electric pressure transducer M. The instantaneous pressure is also indicated by the pressure gage N.

The operating procedure starts with the motorized hydraulic pump P which is used to purge the system of all entrapped air bubbles. The large reservoir tube was incorporated to aid in the air bleeding operation. Then, depending on the mean normal stress to be employed, the appropriate accumulator R was put on the line, and the entire system charged to the given mean pressure with pump K in the central position. The needle valve S was then fully closed, later to be cracked open just slightly such that gage T was able to monitor the mean pressure, while gage N still displayed the instantaneous pressure.

The primary function of the accumulator, of which two were employed in order to cover the test range of mean pressure, was to smooth the system charging process, and subsequently to compensate for leaks without need for recharging. Actual operating experience showed that for most conditions, leaks were no problem, and many tests could be run without having to reopen valve S.

Electrical signals from the strain gages on load transducer B, test specimen A and pressure transducer M were fed to the switch W, from which various combinations of readings could be selected to be plotted by the x-y plotter X. A photograph showing the overall view of the experimental set-up is shown in Figure 2.

III. CALIBRATION ACCURACY AND PRECISION OF APPARATUS

The ideal testing apparatus for this problem would subject the material specimen to axial and internal pressure loadings of perfect sinusoidal waveform applied exactly in phase. The actual test apparatus produced certain distortions in each of the waveforms with consequent phase distortion effects. Since these were inherent deviations of the apparatus, they will be evaluated first.

The waveform distortion stems from the finite connecting rod length of the slider-crank mechanism, which was used, in different forms, in the axial and pressure crank loading devices. The geometries of these two devices are shown in Figure 3(a) and 3(b), from which the displacements x_a and x_p are easily found to be

$$x_a = c + r(1 - \cos \omega t) - \sqrt{c^2 - r^2 \sin^2 \omega t} \quad , \quad (3)$$

$$x_p = -e + \sqrt{e^2 + 2r(r+1)(1 - \cos \omega t)} \quad . \quad (4)$$

The corresponding axial and transverse strains in the specimen are given by

$$\epsilon_1 = m x_a \ell^{-1} + K_1 x_p \quad , \quad (5)$$

$$\epsilon_2 = -\frac{2}{3} m x_a \ell^{-1} + K_2 x_p \quad , \quad (6)$$

where m accounts for the force multiplication of lever E , ℓ is the appropriate specimen length, and K_1 and K_2 account for the fluid pressure coupling between displacement x_p and the test specimen. Substituting the experimentally determined values of m , ℓ , K_1 and K_2 into equations (5), (6), we find

$$10^4 \epsilon_1 = 515 x_a + 1.89 x_p \quad , \quad (7)$$

$$10^4 \epsilon_2 = -129 x_a + 6.61 x_p \quad , \quad (8)$$

where for the values of $c = 14.3$, $e = 25$, and $r = 1.0$ (all in inches) equations (3) and (4) become

$$x_a = 15.3 - \cos \omega t - \sqrt{204.5 - \sin^2 \omega t} \quad , \quad (9)$$

$$x_p = -25 + \sqrt{677 - 52 \cos \omega t} \quad (10)$$

A plot of x_a versus $t = 0$ is shown in Figure 4, which illustrates the amount of waveform distortion present. The corresponding hysteresis loop, obtained by plotting ϵ_1 vs. ϵ_2 , produces a single line, which shows that no loop area is detectable at the level of

precision to be used in the experimental measurements. The precision of the electric strain gage measuring system thus determined the accuracy of the final hysteresis loop.

The disposition of the strain gages on the dynamometer A in Figure 1 is shown in Figure 5. This dynamometer was used for sensing both the axial and pressure loading, with the separate, laboratory standard, pressure transducer M in Figure 1 being used only for calibration checking. The pressure gages were used for visual monitoring only.

The electrical circuitry associated with the transducer was such as to produce individual electric signals directly proportional to ϵ_1 and ϵ_2 [hence, σ_1 and σ_2]. This was achieved by incorporating shunt resistors R_p of 678 ohms [computed theoretically by assuming a Poisson's ration of 1/3 for the transducer material] across the 500 ohm strain gages R_L and R_T in Figure 5.

In order to obtain the desired stresses in the specimen directly, the inside diameter of the specimens was matched to that of the dynamometer. The wall thickness of the specimen was 2.4% of its outside diameter, so that the state of stress was essentially biaxial with a minor third axes compression gradient due to the direct pressure loading. The dimensional detail of the test specimens is shown in Figure 6. The maximum internal pressure was 1000 psi, which produced 20,000 psi axial stress in the walls of the specimen. Hence, the distortional and dilatational strain energies, computed on the basis of a biaxial stress state [$\sigma_1, \sigma_2, \sigma_3 = 0$], were negligibly different from the correct values.

IV. SELECTION OF TEST MATERIAL

Since the objective of this study was concerned with the effects associated with dilatational straining action, it was expedient to eliminate as many as possible of the damping phenomena, nominally a part of the material damping process, but not directly pertinent to dilatational straining. In particular, this meant avoiding problems of stress history, stress amplitude [with reference to cyclic stress sensitivity limit], strain rate [with reference to frequency of loading], test temperature and metallurgical variations of the material.

The material selected for the test specimens was a manganese copper alloy, whose comparatively high damping properties had already been well established with the standard test set-ups, and which thus promised good accuracy of experimental results in the new study. For interest, some specimens were also fabricated from mild steel, but it was discovered that at the low levels of stress which were demanded by the aforementioned considerations

of stress history, etc., the test apparatus had insufficient precision to produce useful results. The manganese copper alloy, with its higher damping, was not observed to have any other unusual characteristics to set it apart from the general category of structural metals.

The manganese copper alloy was obtained in the form of 1 5/8" by 5" bars which were given a normalizing heat treatment by the manufacturer [CDC #780, Chicago Development Corporation, 5810 47th Avenue, Riverdale, Maryland]. The chemical composition and the mechanical properties of this alloy, stated by the manufacturer, were as follows:

<u>Element</u>	<u>Range (% composition)</u>
Manganese	78-82
Copper	18-22
Fatigue Strength	17,000 psi at 10^8 cycles
Modulus of Elasticity	13.5×10^6 psi
0.2% Yield Strength	24,000 psi

Machining and polishing procedures for the test specimens were the same as those described previously in Reference 3.

V. THEORETICAL CONSIDERATIONS WITH RESPECT TO DATA REDUCTION

The specific damping energy absorbed by a material subjected to cyclic, biaxial stress can be determined from the sum of the areas of the two principal stress-strain hysteresis loops. We denote this by

$$D(\sigma_1, \sigma_2) = \oint \sigma_1 d\epsilon_1 + \oint \sigma_2 d\epsilon_2 = D_1 + D_2 ,$$

where σ_1 , σ_2 , and ϵ_1 , ϵ_2 are the principal stresses and strains respectively. If we let the measured areas of the two loops $\sigma_1 - \epsilon_1$ and $\sigma_2 - \epsilon_2$ be A_1 and A_2 respectively, we can write

$$D_1 = N_1 S_1 A_1 , \quad D_2 = N_2 S_2 A_2 ,$$

where N_1 N_2 relate the recorder settings in micro-inches per inch of deflection along the strain axes, and S_1 S_2 relate the settings in psi per inch of deflection along the stress axes, for the individual hysteresis loops. The standard technique utilizing precision shunt resistors in the bridge circuits was used in determining the constants N_1 , N_2 , S_1 , S_2 .

Having evaluated $D(\sigma_1, \sigma_2)$, the next problem is to formulate a reduction which best examines for possible relevance of dilatational strain energy. We note that for the biaxial stress case

$$\text{Distortional Strain Energy} = \bar{U} = \frac{1 + \nu}{3 E} [\sigma_1^2 + \sigma_2^2 - \sigma_1 \sigma_2] ,$$

$$\text{Dilatational Strain Energy} = \bar{U} = \frac{1 - 2\nu}{6 E} [\sigma_1^2 + \sigma_2^2 + 2\sigma_1 \sigma_2] ,$$

from which we find the ratio of the strain energies to be

$$\frac{\bar{U}}{U} = \frac{1 - 2\nu}{2(1 + \nu)} \cdot \frac{(a + 1)^2}{a^2 - a + 1} ,$$

where $a = \sigma_1 / \sigma_2$. A plot of this result is shown in Figure 7(a), where we observe that the stress ratio a is not a convenient parameter for detecting the influence of \bar{U}/U . An alternative parameter is σ_d / τ_m , the ratio of the mean normal to maximum shear stress components, as defined by

$$\sigma_d = \frac{\sigma_1 + \sigma_2}{2} , \quad \tau_m = \frac{\sigma_1 - \sigma_2}{2}$$

In this case we find

$$\frac{\bar{U}}{U} = \frac{1 - 2\nu}{2(1 + \nu)} \cdot \frac{4\beta^2}{\beta^2 + 3}$$

where $\beta = \sigma_d / \tau_m$. A plot of this parameter is shown in Figure 7(b), which is observed to give a simple rising curve for the

energy ratio, and is therefore suitable for our analysis. A third approach is to introduce the notion of effective dilatational and distortional stresses such that

$$\bar{\bar{U}} = \frac{1 - 2\nu}{6 E} \bar{\sigma}^2 ,$$

$$\bar{U} = \frac{1 + \nu}{3 E} \bar{\sigma}^2 .$$

In this case

$$\frac{\bar{\bar{U}}}{\bar{U}} = \frac{1 - 2\nu}{2(1 + \nu)} \left[\frac{\bar{\sigma}}{\bar{\sigma}} \right]^2$$

a plot of which is shown in Figure 7 (c). This latter description is also acceptable, and has the added advantage of covering the entire biaxial stress range in a finite region.

In all of the foregoing plots, we observe that the percentage of dilatational to distortional strain energy which occurs in the uniaxial stress case can be at most increased by a factor of 4 in going to the biaxial stress case. In the case of the manganese copper alloy used in the test specimens, Poisson's ratio equals 0.28, so that the maximum possible value of the energy ratio $\bar{\bar{U}}/\bar{U}$ turned out to be 0.69. Thus, in the biaxial stress case, the magnitude of the dilatational component of the strain energy still falls far short of the distortional component.

We choose the parameter $\bar{\sigma} / \bar{\sigma}$ against which to compare the damping data. More generally, this means working with any two of $\bar{\sigma}$, $\bar{\sigma}$, or $\bar{\sigma} / \bar{\sigma}$.

Several methods of non-dimensionalizing the energy dissipation $D(\sigma_1, \sigma_2)$ can be applied. In particular, if we choose $\bar{\sigma}$ and $\bar{\sigma} / \bar{\sigma}$ as the independent variables, we can write the ratio

$$D(\bar{\sigma}, \bar{\sigma} / \bar{\sigma}) / D(\sigma_n)$$

where $D(\sigma_n)$ represents the energy dissipation which would have been obtained under uniaxial stress conditions with some suitable stress amplitude σ_n . In a similar comparison of data, Whittier [4]

chose to define σ_n as that stress which produced the same distortional energy, which says merely that $\sigma_n = \bar{\sigma}$. An alternative procedure is to use the Robertson-Yorgiadis criterion which says

$$\sigma_n = \sqrt{3} \tau_m = \sqrt{\bar{\sigma}^2 - \frac{1}{4} \bar{\sigma}^2}$$

where τ_m is the maximum shear stress amplitude developed in the biaxial stress state. Actually, Robertson and Yorgiadis found that in the place of $\sqrt{3}$, experimental tests produced values ranging from 1.7 to 2.1. The theoretical basis of $\sqrt{3}$, as noted in the introduction, lies in the (arbitrary) neglect of all effects due to the mean normal stress component σ_d . We will choose to work with the σ_n based on the distortional strain energy, so that we may anticipate plots of the type shown in Figure 8. Thus, if the experimental results follow along curve A, then this would show that the material damping was independent of dilatational straining action. Any slope to the curve, however, would establish a dependence, with curve B demonstrating additive damping effects and curve C a nullifying damping effect. On the other hand, if the material damping depended only on the dilatational straining action, then the data would fall along curve D whose exact position would depend on the individual material.

The foregoing conjecture suggest an alternative plot wherein we use the ratio

$$D(\bar{\sigma}, \bar{\sigma}/\bar{\sigma}) / D(\sigma_n^*)$$

where $\sigma_n^* = \bar{\sigma}$. This is illustrated in Figure 9, wherein insensitivity to distortional straining would produce curve E while insensitivity to dilatational straining would produce curve F.

VI. EXPERIMENTAL RESULTS

The simultaneous loading of the specimen by two loading systems required continual checking to see that no phase discrepancy developed, which, of course, would produce false hysteresis loops. The technique employed was to monitor σ_1 versus σ_2 in all cases, in addition to the required hysteresis loops σ_1 versus ϵ_1 σ_2 versus ϵ_2 . If the plot of σ_1 versus σ_2 did not produce a

straight line (loop of zero area), then the mechanical coupling between the axial and pressure loading cranks was adjusted until a straight line was produced. Elastic deformation of the loading system made such adjustment necessary for almost all changes of loading amplitudes, with the maximum adjustment reaching $+10^\circ$ from the zero load, in phase position. Two typical sets of loops, including also a plot of ϵ_1 versus ϵ_2 , are shown in Figures 10 and 11.

The test range of σ_a and σ_t , the amplitudes of the axial and transverse cyclic components of stress, was limited at the lower end by the ability to determine the loop areas with a planimeter to within 10 to 15%, and at the high end by the onset of stress history effects. In the case of the manganese copper alloy test specimens, this meant that the mean pressure in the hydraulic loading system was kept in the range 600 to 700 psi with the minimum pressure falling to not less than 300 psi. The axial load was restricted to remain either negative or positive at all parts of the cycle and to produce a maximum 20,000 psi axial stress. At least one of the σ_1 or σ_2 had to be not less than 5000 psi in order to generate hysteresis loops of acceptable area. A typical check for the absence of stress history effects is shown in figure 12 for uniaxial tension, and in Figure 13 for a biaxial stress case.

The formal experimental test program was carried out on five specimens. Over 400 test runs were made on these specimens, hence we omit their numerical tabulation and present only the reduced results in the form of plots. In the case of specimen A, we show the two type of plots corresponding to Figures 8 and 9, in Figures 14 and 15. It is clear that the first of these plots is to be preferred, hence this presentation only is used for specimens B, C, D and E in Figures 16, 17, 18 and 19. The uniaxial damping data were determined (experimentally) individually for all specimens for the given reductions of data, an example of which has already been shown in Figure 12 in connection with stress history effects.

VII. DISCUSSION OF RESULTS AND CONCLUSIONS

The basic result of the tests reported herein is the observation that the experimental plots tend to favor the curve (b) in Figure 9. Considerable scatter of results, both test-to-test and specimen-to-specimen is evident, but this is usual, even for the carefully prepared specimens which were employed. The conclusion is therefore, that attention to the dilatational strain energy is necessary in considering material damping in the alloy tested. Except for very special materials, this has not been a generally

accepted notion, at least for structural metals, although some recent work on the vibrations of circular plates has also indicated this [4]. This latter study, however, involved a highly non-uniform stress distribution, so that its quantitative interpretation was subject to substantial error. The present study, of course, has employed a uniform state of stress with full control over stress ratios, so that with the neglect of the small stress component through the wall thickness, the results are direct.

It is observed that if an attempt were made to fit the data in Figures 15, 17, 18, 19 and 20 with smooth curves, then the intersections at

$$\bar{\sigma} / \sigma = 1$$

would be at 1.0, 0.8, 1.1, 1.0 and 1.2 for the five specimens. All of these ordinates would be expected to be 1.0, but once again, apparently only the statistical answer satisfies the expected behavior.

Finally, we observe, that if the non-dimensionalization had been made with the Robertson-Yorgiadis criterion, then the positive slopes shown by the foregoing curves would have been greater. The significance of dilatational straining action on material damping therefore appears to be established, and this calls for a modification of the elementary, distortional energy criterion (based on maximum shear stress) for relating uniaxial with biaxial stress states which produce the same damping. The purpose of such criterion, of course, is to allow determination of material damping under any biaxial state of stress, given the value in one state. In particular, if we choose the modified criterion as given by Equation 1 and use a straight line description of the experimental results in Figure 15, and furthermore, note that the material damping for manganese copper alloys behaves like $\sigma_n^{2.8}$ in the uniaxial case, we find that required value of λ is 1.2. If the material should behave primarily in accordance with the Robertson-Yorgiadis criterion, then the reformulation to account for dilatational straining would take the form

$$\sigma_n = \sqrt{(3 - \lambda^*) \tau_m^2 + \lambda^* \sigma_d^2},$$

so that, under uniaxial stress conditions, wherein $\tau_m = \sigma_d$, the expression reverts to $\sigma_n = \sqrt{3} \tau_m$.

VIII. REFERENCES

1. Robertson, J. M. and Yorgiadis, A. J., "Internal Friction in Engineering Materials," Journal of Applied Mechanics, Vol. 13, 1946.
2. Mentel, T. J., "Vibrational Energy Dissipation at Structural Support Junctions," Section 4 of, "Structural Damping," Edited by J. E. Ruzicka, ASME, 1959.
3. Lazan, B. J., "A Study with New Equipment of the Effects of Fatigue Stress on the Damping Capacity and Elasticity of Mild Steel," Transactions ASME, Vol. 4, 1950.
4. Whittier, J. S., "Phenomenological Theories of Hysteretic Material Damping with Application to the Vibrations of Circular Plates," ASD Technical Report 61-264, November 1961.

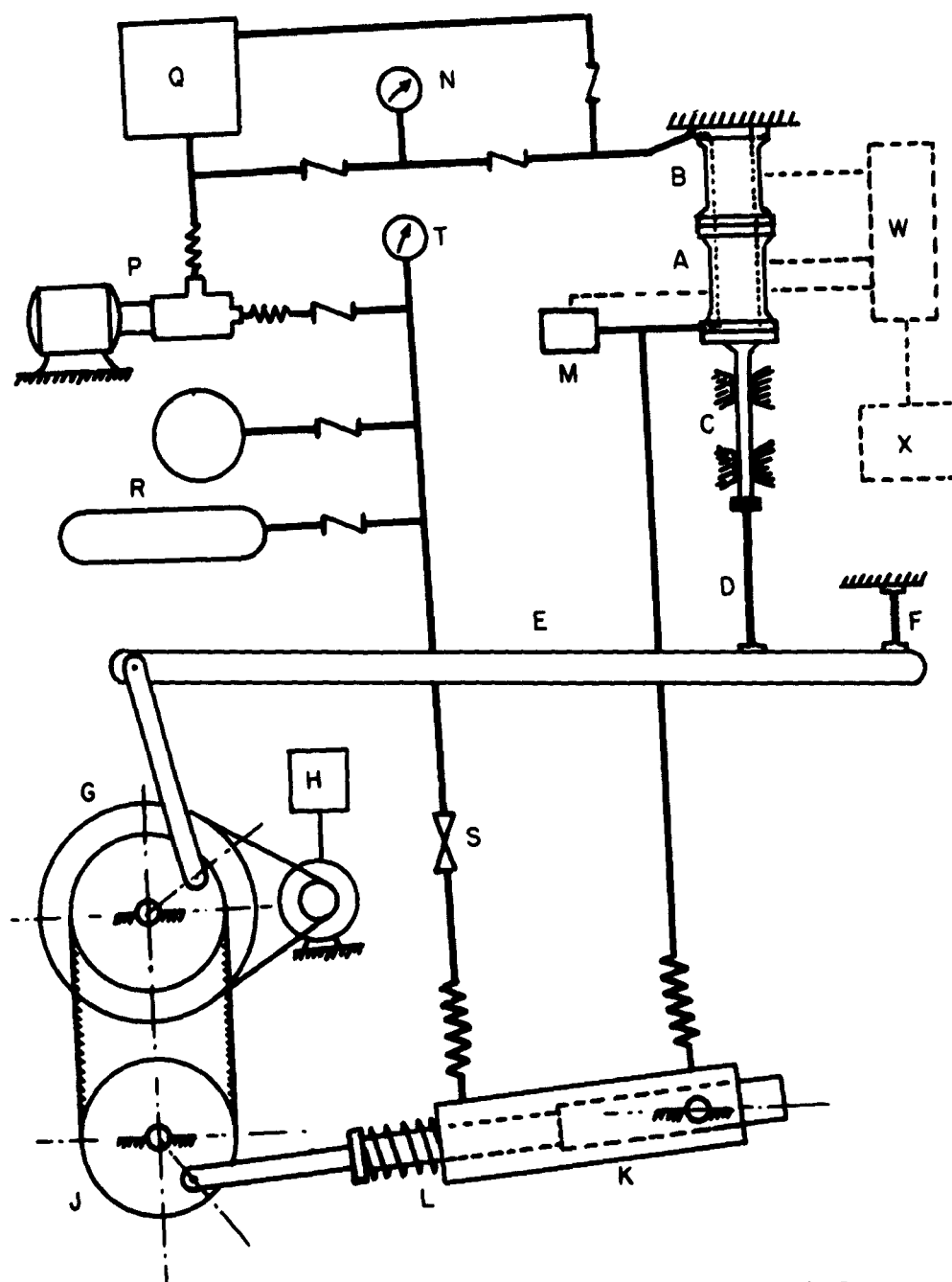


Figure 1. - Schematic of Test Apparatus

LEGEND FOR FIGURE I

A	Test specimen
B	Load transducer
C	Vertical guide
D	Axial load transfer lever
E, D	Flexible couplings
G, J	Axial load and internal pressure cranks
H	Speed control
K	Pressure loading jack
L	Mean load relief spring
M	Precision pressure transducer
N, T	Pressure gages
P	Hydraulic pump
Q	Reservoir
R	Hydraulic pressure accumulators
S	Needle valve
W	Switch box
X	X-Y plotter

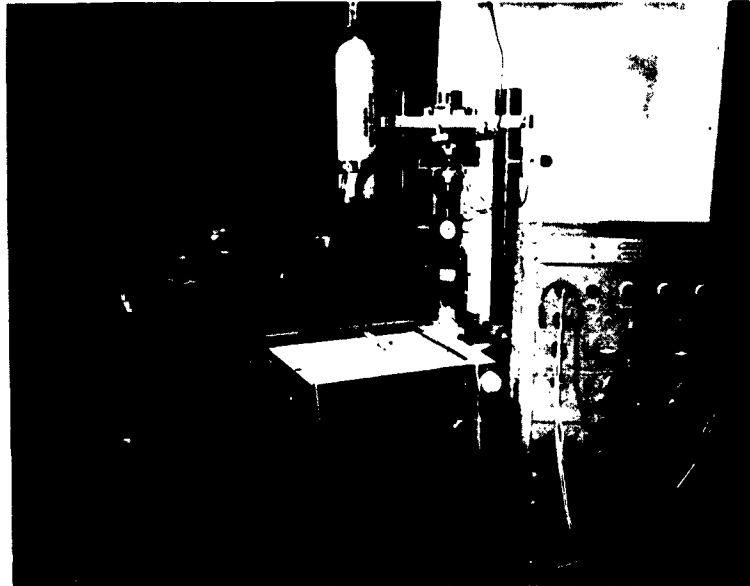
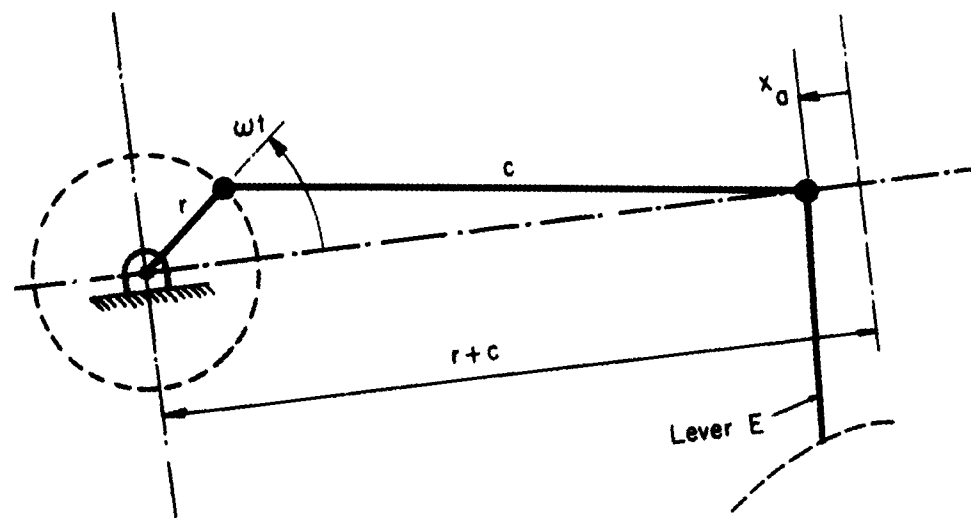
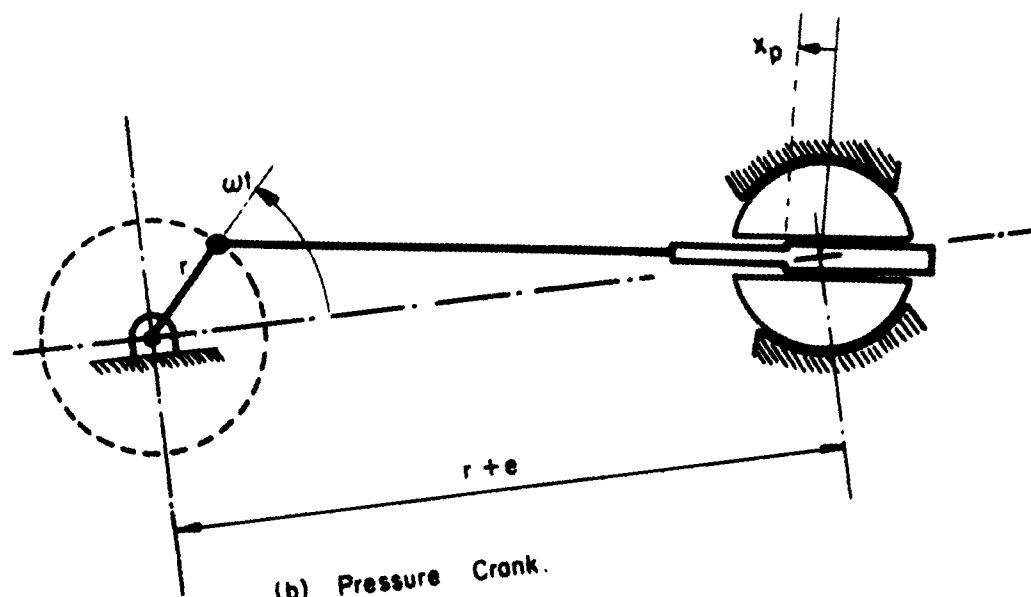


Figure 2. - Overall Test Set-Up



(a) Axial Crank



(b) Pressure Crank.

Figure 3. - Axial and Pressure Crank Geometries

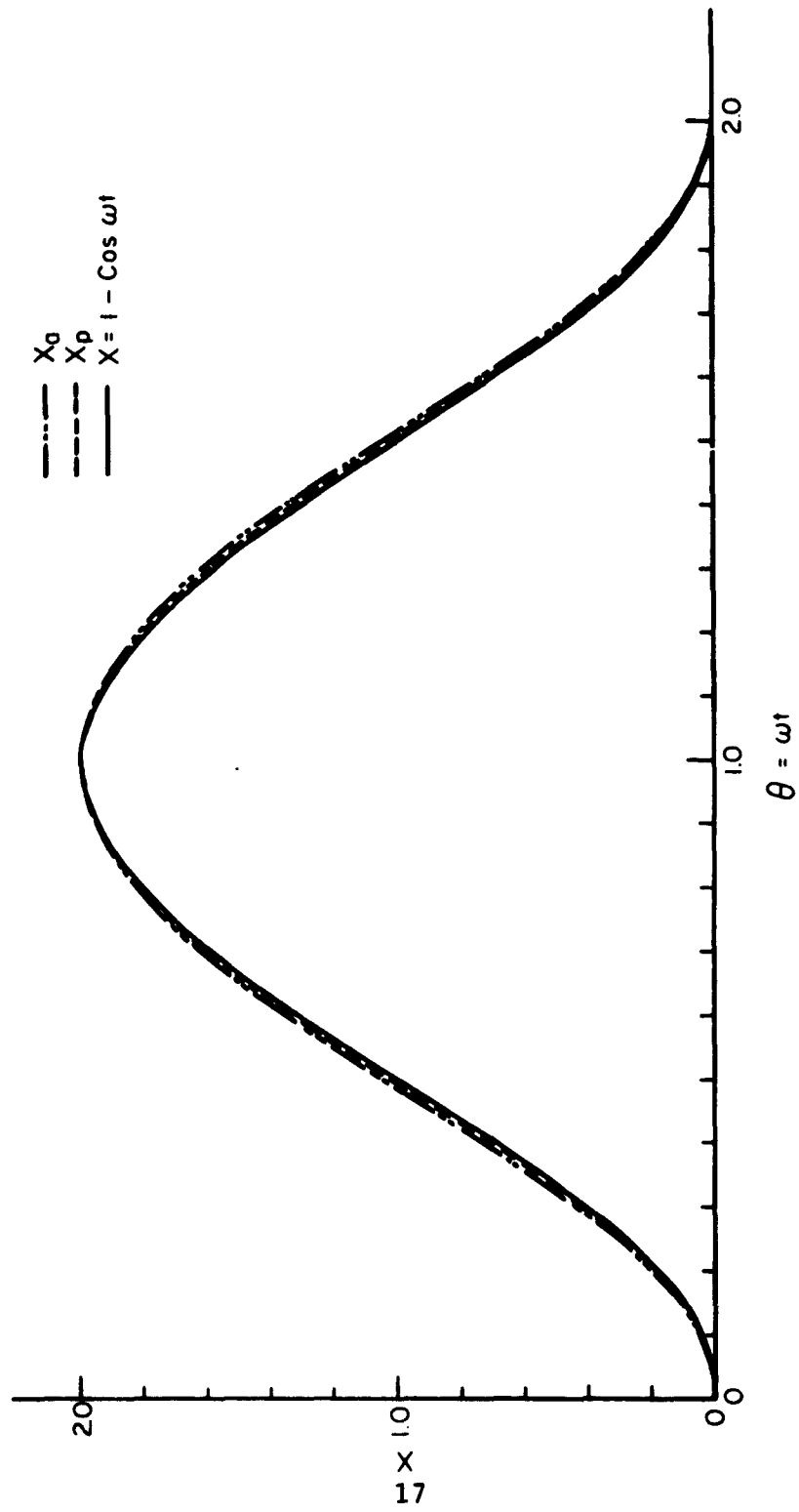
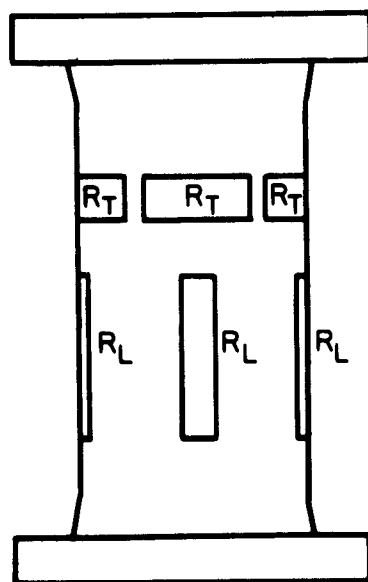
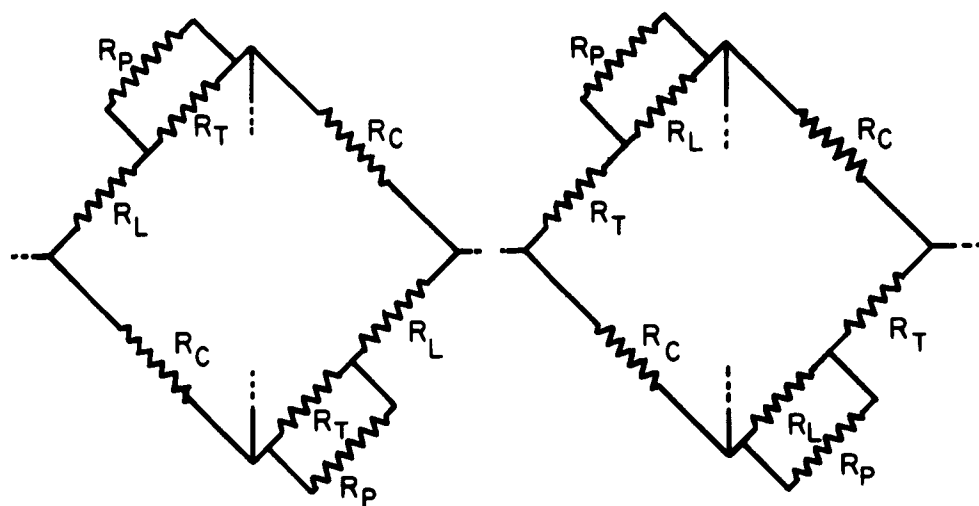


Figure 4. - Displacement Waveform Distortion



- R_L - Longitudinal gage
- R_T - Transverse gage
- R_P - Precision resistor
- R_C - Compensating gage

Figure 5. - Strain Gage Disposition and Bridge Set-Ups

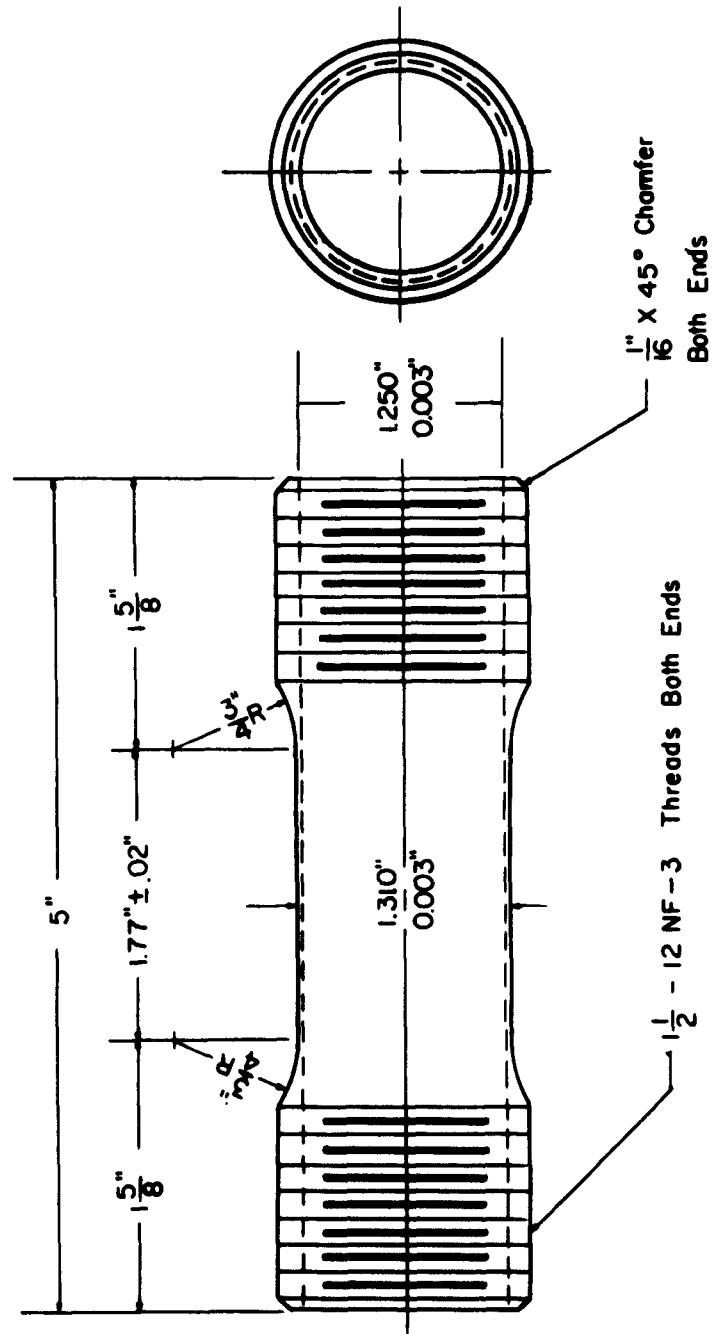


Figure 6. - Geometry of Test Specimens

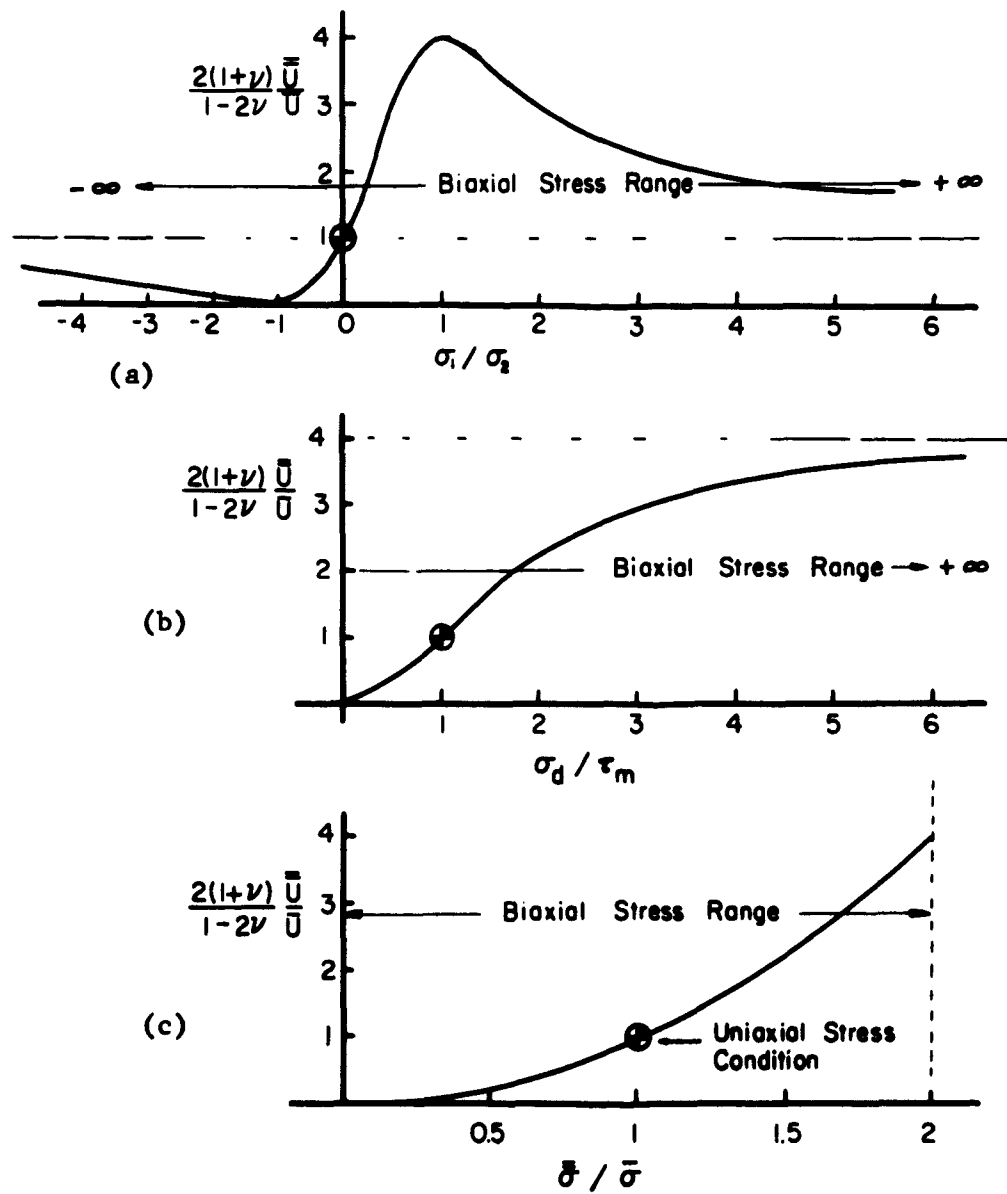


Figure 7. - Comparison of Parameters for
Depicting Energy Ratios

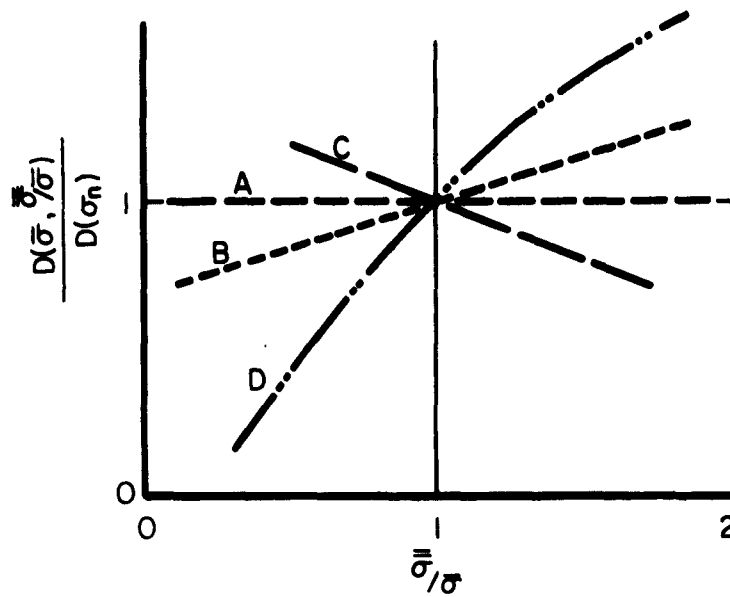


Figure 8. - Basic Trend Curves for Material Damping

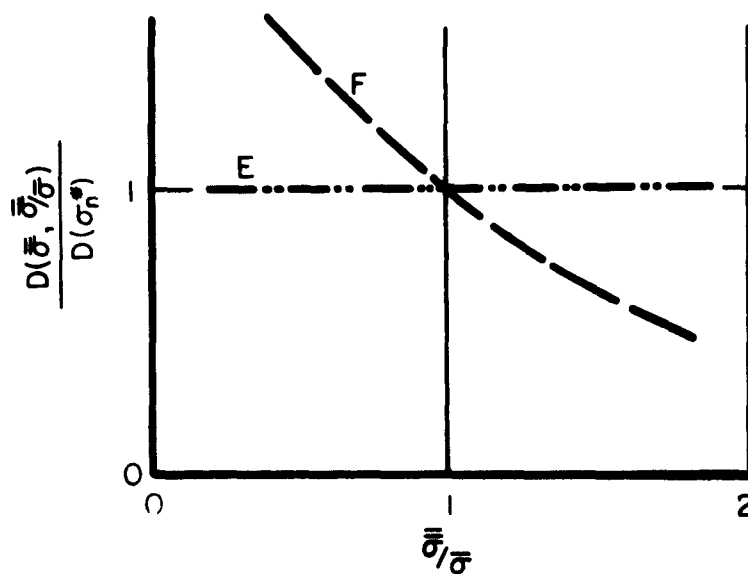


Figure 9 - Alternate Presentation of Trend Curves

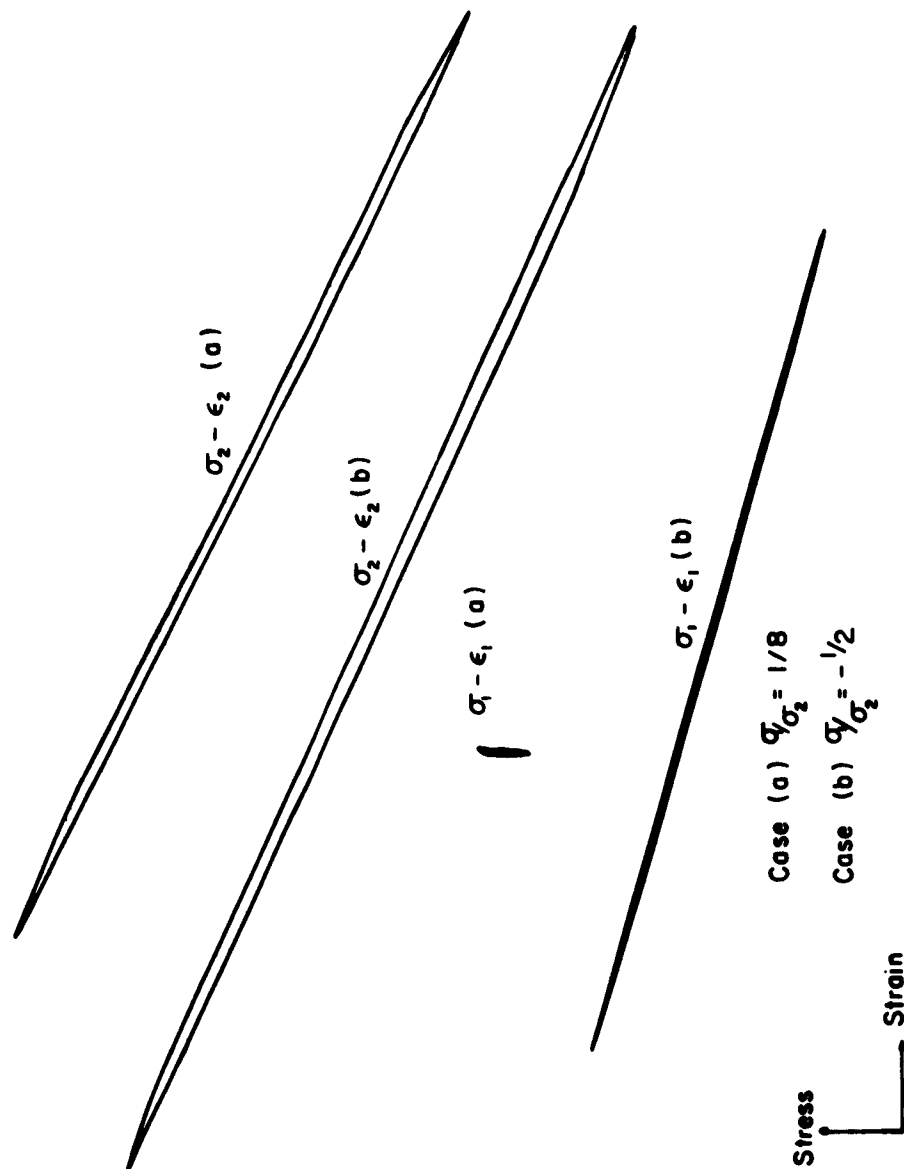


Figure 10. - Typical Hysteresis Loops

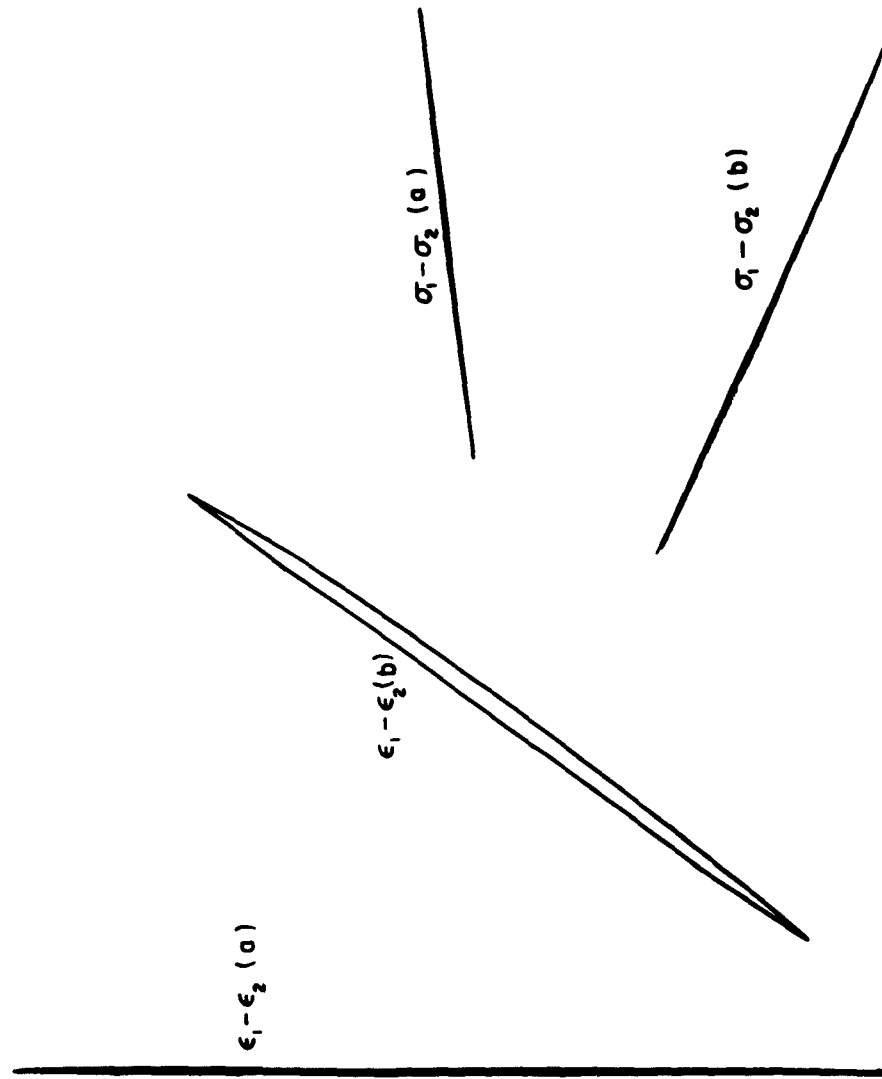


Figure 11. - Typical Phase-Check Loops Corresponding to Figure 11

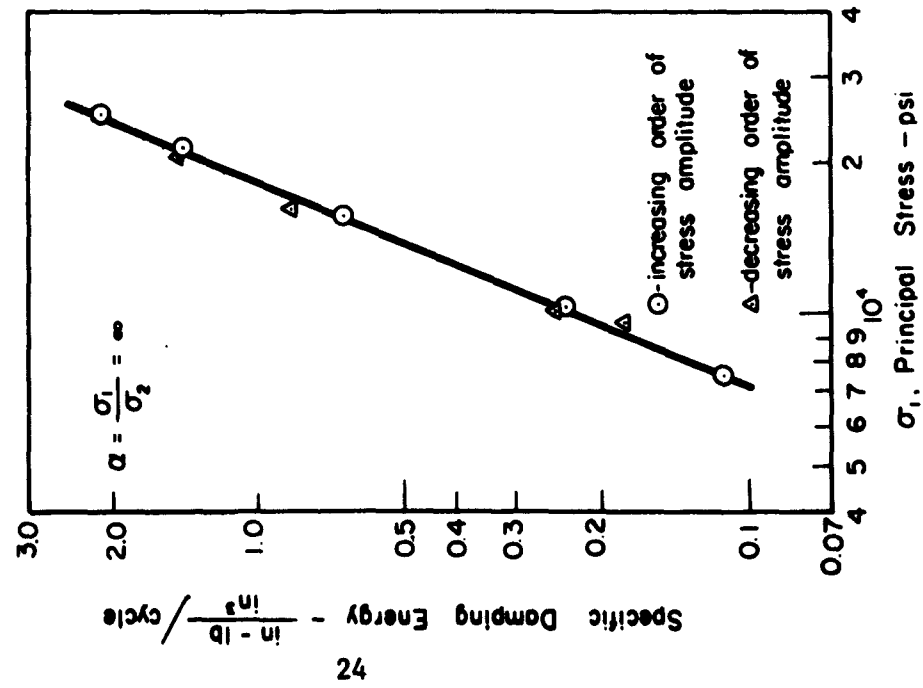


Figure 12. - Stress History Check with Uniaxial Stress

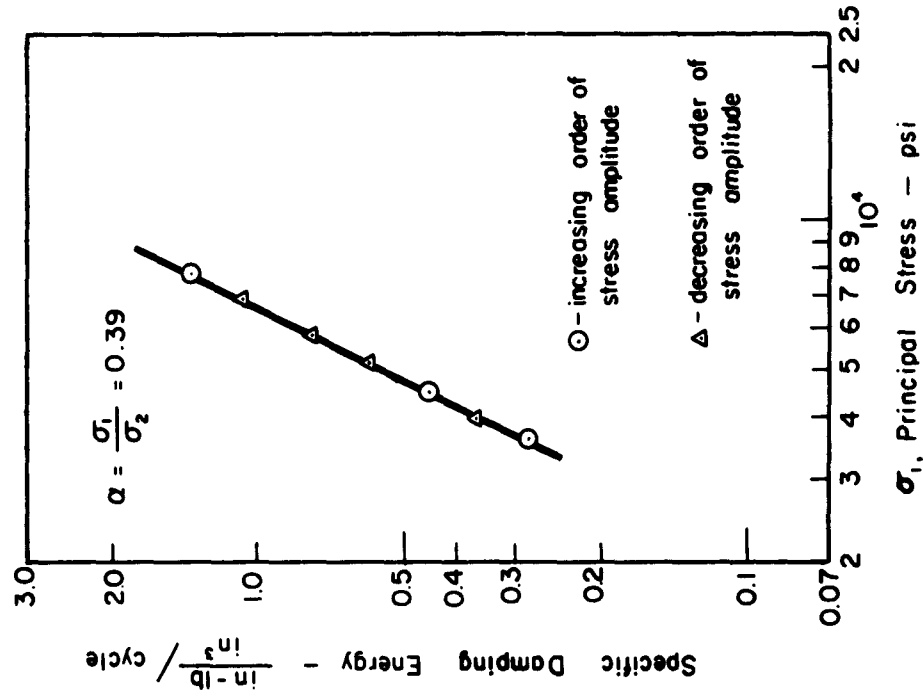


Figure 13. - Stress History Check with Biaxial Stress

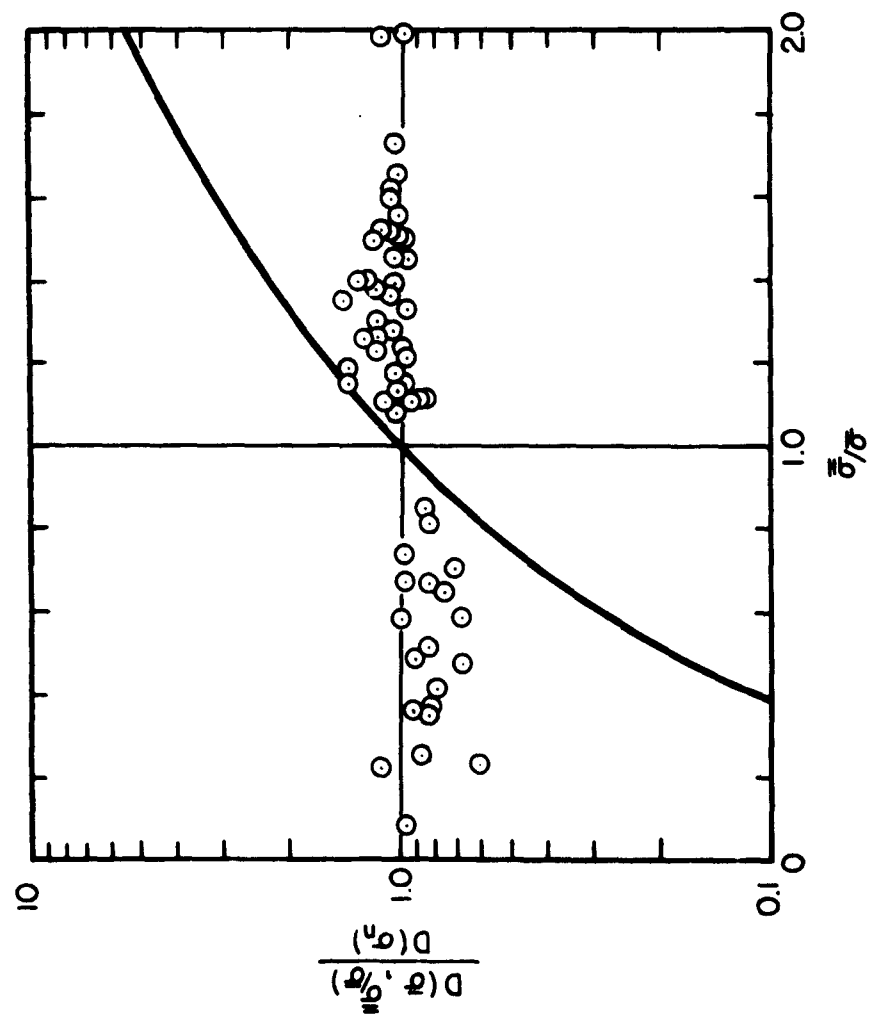


Figure 14. - Experimental Results, Specimen A

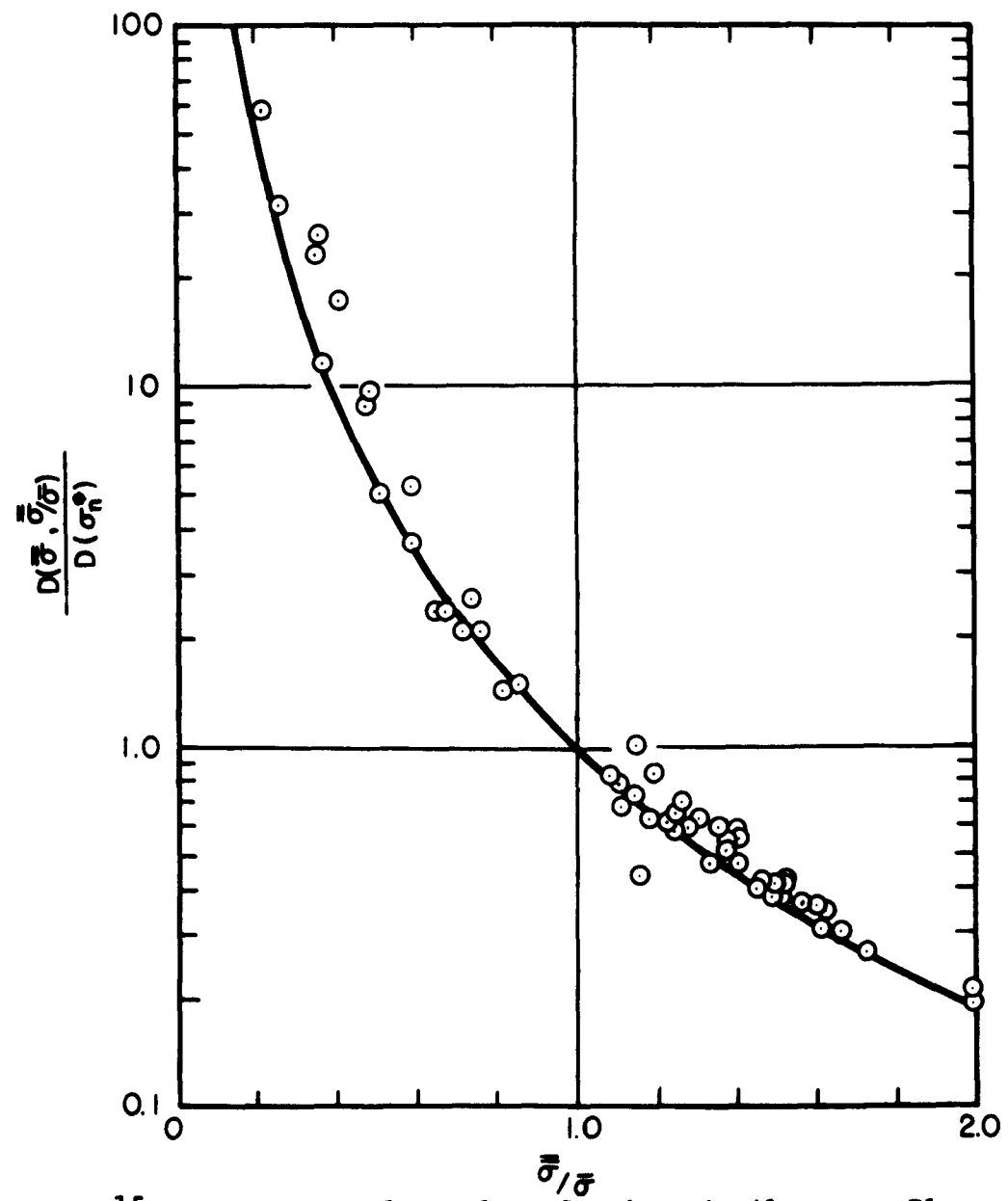


Figure 15. - Experimental Results, Specimen A, Alternate Plot

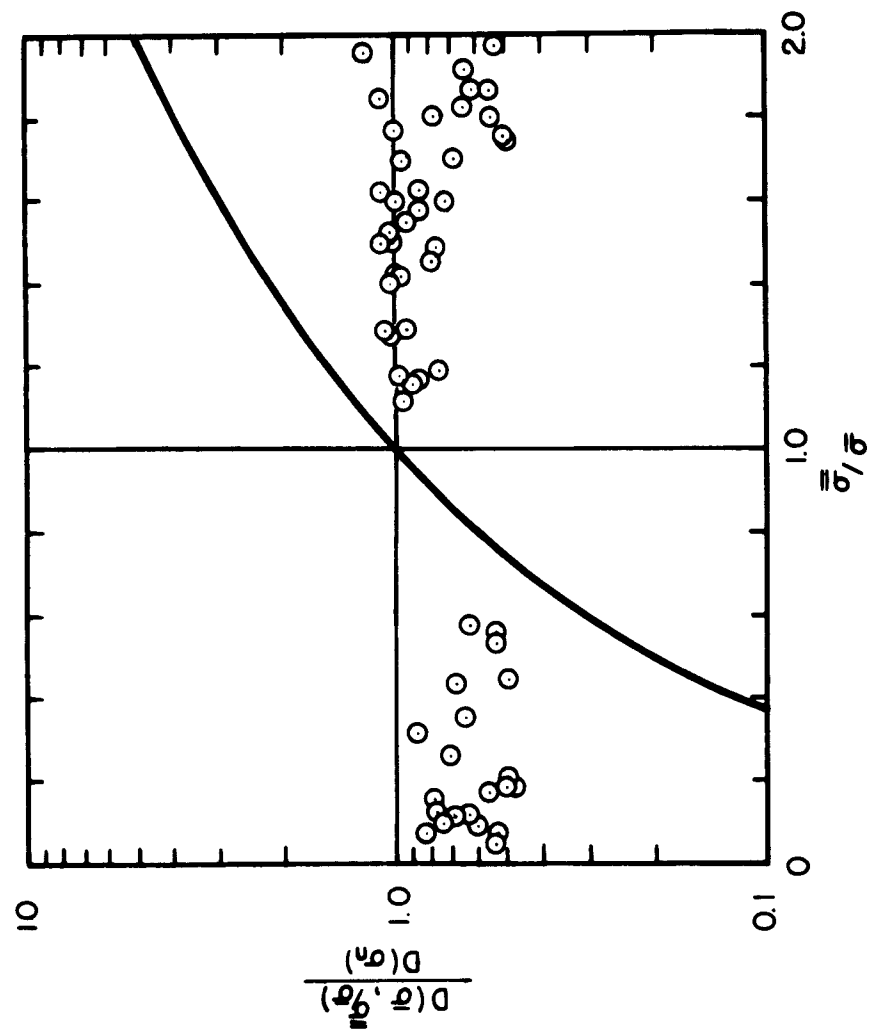


Figure 16. - Experimental Results, Specimen B

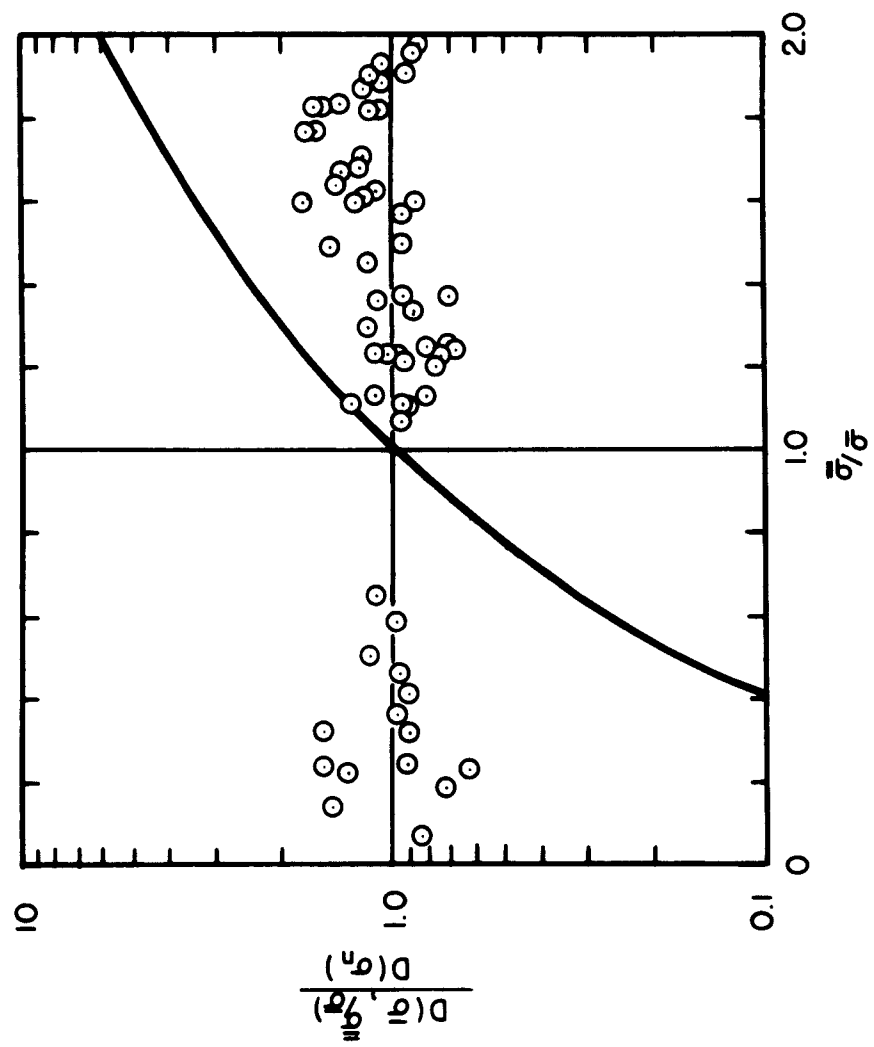


Figure 17. - Experimental Results, Specimen C

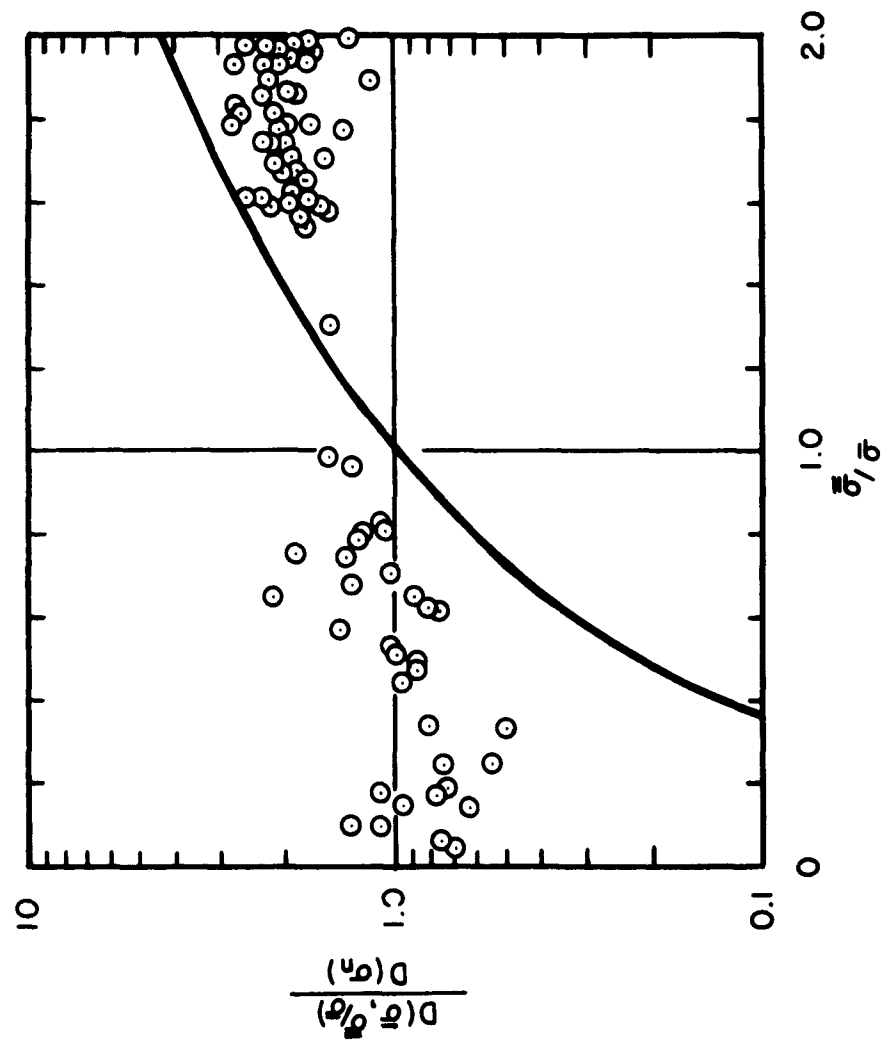


Figure 18. - Experimental Results, Specimen D

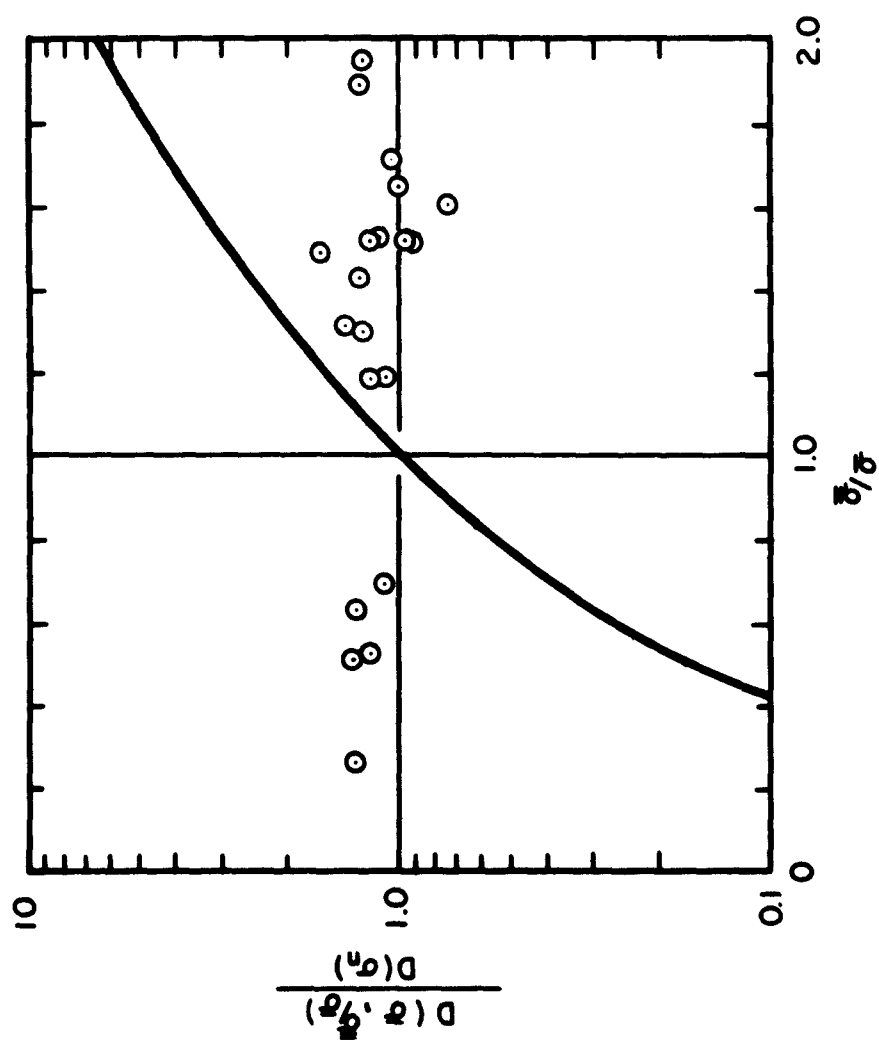


Figure 19. - Experimental Results, Specimen E

Aeronautical Systems Division, AF Materie
Laboratory, Metals and Ceramics Division,
Wright-Patterson AFB, Ohio.

Rpt No. ASD-STR-63-497. MATERIAL DAMPING
UNDER BIAXIAL STRESS OF STRESS GENERATED BY
COMBINED AXIAL AND INTERNAL PRESSURE
LOADINGS. Final report, July 63. 30pp.
incl illus., tables, & refs..

Unclassified Report

A test machine has been constructed which
measures material damping in thin-walled,
cylindrical specimens subject to combined
internal pressure and axial cyclic loading.
The purpose of this machine is to allow the
complete range of biaxial stress states to
be developed, so that the individual damping
effects of distortional and dilatational

(over)

straining action might be clearly discerned.
Experimental results on a series of mag-
nes alloy specimens are found to display
significant damping effect associated with
dilatational straining.

ASD-STR-63-497

1. Material damping
2. Mechanical prop-
erties

3. Biaxial stress
4. Biaxial stress
damping apparatus
1. AFRC Project 7351,
Task 735106

II. Contract No.
AF 33(657)-7453

III. University of
Minnesota, Min-
neapolis, Minn.
IV. T. J. Mental
S. H. Chi

V. Avail fr OPS
VI. In ASTIA collec-
tion

Aeronautical Systems Division, AF Materie
Laboratory, Metals and Ceramics Division,
Wright-Patterson AFB, Ohio.

Rpt No. ASD-STR-63-497. MATERIAL DAMPING
UNDER BIAXIAL STRESS OF STRESS GENERATED BY
COMBINED AXIAL AND INTERNAL PRESSURE
LOADINGS. Final report, July 63. 30pp.
incl illus., tables, & refs..

Unclassified Report

A test machine has been constructed which
measures material damping in thin-walled,
cylindrical specimens subject to combined
internal pressure and axial cyclic loading.
The purpose of this machine is to allow the
complete range of biaxial stress states to
be developed, so that the individual damping
effects of distortional and dilatational

(over)

straining action might be clearly discerned.
Experimental results on a series of mag-
nes alloy specimens are found to display
significant damping effect associated with
dilatational straining.

ASD-STR-63-497

Aeronautical Systems Division, AF Materials Laboratory, Metals and Ceramics Division, Wright-Patterson AFB, Ohio.
Rpt No. ASD-TDR-63-647. MATERIAL DAMPING UNDER BIAXIAL STATE OF STRESS GENERATED BY COMBINED AXIAL AND INTERNAL PRESSURE LOADINGS. Final report, July 63. 30pp. Incl illus., tables, & refs..
Unclassified Report

A test machine has been constructed which measures material damping in thin-walled, cylindrical specimens subject to combined internal pressure and axial cyclic loading. The purpose of this machine is to allow the complete range of biaxial stress states to be developed, so that the individual damping effect, of distortional and dilatational

straining action might be clearly discerned. Experimental results on a series of manganese alloy specimens are found to display significant damping effect associated with dilatational straining.

ASD-TDR-63-647

1. Material damping
2. Mechanical properties
3. Biaxial stress
4. Biaxial stress damping apparatus
I. AFSC Project 7351, Task 735106
II. Contract No.
AP 33(657)-7453
III. University of Minnesota, Minneapolis, Minn.
IV. T. J. Mentel
S. H. Chi
V. Avail fr OTS
VI. In ASTIA collection

Aeronautical Systems Division, AF Materials Laboratory, Metals and Ceramics Division, Wright-Patterson AFB, Ohio.
Rpt No. ASD-TDR-63-647. MATERIAL DAMPING UNDER BIAXIAL STATE OF STRESS GENERATED BY COMBINED AXIAL AND INTERNAL PRESSURE LOADINGS. Final report, July 63. 30pp. Incl illus., tables, & refs..
Unclassified Report

A test machine has been constructed which measures material damping in thin-walled, cylindrical specimens subject to combined internal pressure and axial cyclic loading. The purpose of this machine is to allow the complete range of biaxial stress states to be developed, so that the individual damping effect, of distortional and dilatational

straining action might be clearly discerned. Experimental results on a series of manganese alloy specimens are found to display significant damping effect associated with dilatational straining.

ASD-TDR-63-647

1. Material damping
2. Mechanical properties
3. Biaxial stress
4. Biaxial stress damping apparatus
I. AFSC Project 7351, Task 735106
II. Contract No.
AP 33(657)-7453
III. University of Minnesota, Minneapolis, Minn.
IV. T. J. Mentel
S. H. Chi
V. Avail fr OTS
VI. In ASTIA collection

(over)

(over)

<p>Aeronautical Systems Division, AF Materials Laboratory, Metals and Ceramics Division, Wright-Patterson AFB, Ohio.</p> <p>REP No. AND-TR-63-47. MATERIAL DAMPING UNDER BIAXIAL STRESS OF STRESS GENERATED BY COMBINED AXIAL AND INTERNAL PRESSURE LOADINGS. Final report, July 63. 30pp. Incl illus., tables, & refs..</p> <p>Unclassified Report</p> <p>A test machine has been constructed which measures material damping in thin-walled, cylindrical specimens subject to combined internal pressure and axial cyclic loading. The purpose of this machine is to allow the complete range of biaxial stress states to be developed, so that the individual damping effects of distortional and dilatational</p>	<p>1. Material damping</p> <p>2. Mechanical properties</p> <p>3. Biaxial stress</p> <p>4. Biaxial stress</p> <p>5. Biaxial stress</p> <p>6. Biaxial stress</p> <p>7. Biaxial stress</p> <p>8. Biaxial stress</p> <p>9. Biaxial stress</p> <p>10. Biaxial stress</p> <p>11. Biaxial stress</p> <p>12. Biaxial stress</p> <p>13. Biaxial stress</p> <p>14. Biaxial stress</p> <p>15. Biaxial stress</p> <p>16. Biaxial stress</p> <p>17. Biaxial stress</p> <p>18. Biaxial stress</p> <p>19. Biaxial stress</p> <p>20. Biaxial stress</p> <p>21. Biaxial stress</p> <p>22. Biaxial stress</p> <p>23. Biaxial stress</p> <p>24. Biaxial stress</p> <p>25. Biaxial stress</p> <p>26. Biaxial stress</p> <p>27. Biaxial stress</p> <p>28. Biaxial stress</p> <p>29. Biaxial stress</p> <p>30. Biaxial stress</p> <p>31. Biaxial stress</p> <p>32. Biaxial stress</p> <p>33. Biaxial stress</p> <p>34. Biaxial stress</p> <p>35. Biaxial stress</p> <p>36. Biaxial stress</p> <p>37. Biaxial stress</p> <p>38. Biaxial stress</p> <p>39. Biaxial stress</p> <p>40. Biaxial stress</p> <p>41. Biaxial stress</p> <p>42. Biaxial stress</p> <p>43. Biaxial stress</p> <p>44. Biaxial stress</p> <p>45. Biaxial stress</p> <p>46. Biaxial stress</p> <p>47. Biaxial stress</p> <p>48. Biaxial stress</p> <p>49. Biaxial stress</p> <p>50. Biaxial stress</p> <p>51. Biaxial stress</p> <p>52. Biaxial stress</p> <p>53. Biaxial stress</p> <p>54. Biaxial stress</p> <p>55. Biaxial stress</p> <p>56. Biaxial stress</p> <p>57. Biaxial stress</p> <p>58. Biaxial stress</p> <p>59. Biaxial stress</p> <p>60. Biaxial stress</p> <p>61. Biaxial stress</p> <p>62. Biaxial stress</p> <p>63. Biaxial stress</p> <p>64. Biaxial stress</p> <p>65. Biaxial stress</p> <p>66. Biaxial stress</p> <p>67. Biaxial stress</p> <p>68. Biaxial stress</p> <p>69. Biaxial stress</p> <p>70. Biaxial stress</p> <p>71. Biaxial stress</p> <p>72. Biaxial stress</p> <p>73. Biaxial stress</p> <p>74. Biaxial stress</p> <p>75. Biaxial stress</p> <p>76. Biaxial stress</p> <p>77. Biaxial stress</p> <p>78. Biaxial stress</p> <p>79. Biaxial stress</p> <p>80. Biaxial stress</p> <p>81. Biaxial stress</p> <p>82. Biaxial stress</p> <p>83. Biaxial stress</p> <p>84. Biaxial stress</p> <p>85. Biaxial stress</p> <p>86. Biaxial stress</p> <p>87. Biaxial stress</p> <p>88. Biaxial stress</p> <p>89. Biaxial stress</p> <p>90. Biaxial stress</p> <p>91. Biaxial stress</p> <p>92. Biaxial stress</p> <p>93. Biaxial stress</p> <p>94. Biaxial stress</p> <p>95. Biaxial stress</p> <p>96. Biaxial stress</p> <p>97. Biaxial stress</p> <p>98. Biaxial stress</p> <p>99. Biaxial stress</p> <p>100. Biaxial stress</p>	<p>1. Material damping</p> <p>2. Mechanical properties</p> <p>3. Biaxial stress</p> <p>4. Biaxial stress</p> <p>5. Biaxial stress</p> <p>6. Biaxial stress</p> <p>7. Biaxial stress</p> <p>8. Biaxial stress</p> <p>9. Biaxial stress</p> <p>10. Biaxial stress</p> <p>11. Biaxial stress</p> <p>12. Biaxial stress</p> <p>13. Biaxial stress</p> <p>14. Biaxial stress</p> <p>15. Biaxial stress</p> <p>16. Biaxial stress</p> <p>17. Biaxial stress</p> <p>18. Biaxial stress</p> <p>19. Biaxial stress</p> <p>20. Biaxial stress</p> <p>21. Biaxial stress</p> <p>22. Biaxial stress</p> <p>23. Biaxial stress</p> <p>24. Biaxial stress</p> <p>25. Biaxial stress</p> <p>26. Biaxial stress</p> <p>27. Biaxial stress</p> <p>28. Biaxial stress</p> <p>29. Biaxial stress</p> <p>30. Biaxial stress</p> <p>31. Biaxial stress</p> <p>32. Biaxial stress</p> <p>33. Biaxial stress</p> <p>34. Biaxial stress</p> <p>35. Biaxial stress</p> <p>36. Biaxial stress</p> <p>37. Biaxial stress</p> <p>38. Biaxial stress</p> <p>39. Biaxial stress</p> <p>40. Biaxial stress</p> <p>41. Biaxial stress</p> <p>42. Biaxial stress</p> <p>43. Biaxial stress</p> <p>44. Biaxial stress</p> <p>45. Biaxial stress</p> <p>46. Biaxial stress</p> <p>47. Biaxial stress</p> <p>48. Biaxial stress</p> <p>49. Biaxial stress</p> <p>50. Biaxial stress</p> <p>51. Biaxial stress</p> <p>52. Biaxial stress</p> <p>53. Biaxial stress</p> <p>54. Biaxial stress</p> <p>55. Biaxial stress</p> <p>56. Biaxial stress</p> <p>57. Biaxial stress</p> <p>58. Biaxial stress</p> <p>59. Biaxial stress</p> <p>60. Biaxial stress</p> <p>61. Biaxial stress</p> <p>62. Biaxial stress</p> <p>63. Biaxial stress</p> <p>64. Biaxial stress</p> <p>65. Biaxial stress</p> <p>66. Biaxial stress</p> <p>67. Biaxial stress</p> <p>68. Biaxial stress</p> <p>69. Biaxial stress</p> <p>70. Biaxial stress</p> <p>71. Biaxial stress</p> <p>72. Biaxial stress</p> <p>73. Biaxial stress</p> <p>74. Biaxial stress</p> <p>75. Biaxial stress</p> <p>76. Biaxial stress</p> <p>77. Biaxial stress</p> <p>78. Biaxial stress</p> <p>79. Biaxial stress</p> <p>80. Biaxial stress</p> <p>81. Biaxial stress</p> <p>82. Biaxial stress</p> <p>83. Biaxial stress</p> <p>84. Biaxial stress</p> <p>85. Biaxial stress</p> <p>86. Biaxial stress</p> <p>87. Biaxial stress</p> <p>88. Biaxial stress</p> <p>89. Biaxial stress</p> <p>90. Biaxial stress</p> <p>91. Biaxial stress</p> <p>92. Biaxial stress</p> <p>93. Biaxial stress</p> <p>94. Biaxial stress</p> <p>95. Biaxial stress</p> <p>96. Biaxial stress</p> <p>97. Biaxial stress</p> <p>98. Biaxial stress</p> <p>99. Biaxial stress</p> <p>100. Biaxial stress</p>	<p>1. Material damping</p> <p>2. Mechanical properties</p> <p>3. Biaxial stress</p> <p>4. Biaxial stress</p> <p>5. Biaxial stress</p> <p>6. Biaxial stress</p> <p>7. Biaxial stress</p> <p>8. Biaxial stress</p> <p>9. Biaxial stress</p> <p>10. Biaxial stress</p> <p>11. Biaxial stress</p> <p>12. Biaxial stress</p> <p>13. Biaxial stress</p> <p>14. Biaxial stress</p> <p>15. Biaxial stress</p> <p>16. Biaxial stress</p> <p>17. Biaxial stress</p> <p>18. Biaxial stress</p> <p>19. Biaxial stress</p> <p>20. Biaxial stress</p> <p>21. Biaxial stress</p> <p>22. Biaxial stress</p> <p>23. Biaxial stress</p> <p>24. Biaxial stress</p> <p>25. Biaxial stress</p> <p>26. Biaxial stress</p> <p>27. Biaxial stress</p> <p>28. Biaxial stress</p> <p>29. Biaxial stress</p> <p>30. Biaxial stress</p> <p>31. Biaxial stress</p> <p>32. Biaxial stress</p> <p>33. Biaxial stress</p> <p>34. Biaxial stress</p> <p>35. Biaxial stress</p> <p>36. Biaxial stress</p> <p>37. Biaxial stress</p> <p>38. Biaxial stress</p> <p>39. Biaxial stress</p> <p>40. Biaxial stress</p> <p>41. Biaxial stress</p> <p>42. Biaxial stress</p> <p>43. Biaxial stress</p> <p>44. Biaxial stress</p> <p>45. Biaxial stress</p> <p>46. Biaxial stress</p> <p>47. Biaxial stress</p> <p>48. Biaxial stress</p> <p>49. Biaxial stress</p> <p>50. Biaxial stress</p> <p>51. Biaxial stress</p> <p>52. Biaxial stress</p> <p>53. Biaxial stress</p> <p>54. Biaxial stress</p> <p>55. Biaxial stress</p> <p>56. Biaxial stress</p> <p>57. Biaxial stress</p> <p>58. Biaxial stress</p> <p>59. Biaxial stress</p> <p>60. Biaxial stress</p> <p>61. Biaxial stress</p> <p>62. Biaxial stress</p> <p>63. Biaxial stress</p> <p>64. Biaxial stress</p> <p>65. Biaxial stress</p> <p>66. Biaxial stress</p> <p>67. Biaxial stress</p> <p>68. Biaxial stress</p> <p>69. Biaxial stress</p> <p>70. Biaxial stress</p> <p>71. Biaxial stress</p> <p>72. Biaxial stress</p> <p>73. Biaxial stress</p> <p>74. Biaxial stress</p> <p>75. Biaxial stress</p> <p>76. Biaxial stress</p> <p>77. Biaxial stress</p> <p>78. Biaxial stress</p> <p>79. Biaxial stress</p> <p>80. Biaxial stress</p> <p>81. Biaxial stress</p> <p>82. Biaxial stress</p> <p>83. Biaxial stress</p> <p>84. Biaxial stress</p> <p>85. Biaxial stress</p> <p>86. Biaxial stress</p> <p>87. Biaxial stress</p> <p>88. Biaxial stress</p> <p>89. Biaxial stress</p> <p>90. Biaxial stress</p> <p>91. Biaxial stress</p> <p>92. Biaxial stress</p> <p>93. Biaxial stress</p> <p>94. Biaxial stress</p> <p>95. Biaxial stress</p> <p>96. Biaxial stress</p> <p>97. Biaxial stress</p> <p>98. Biaxial stress</p> <p>99. Biaxial stress</p> <p>100. Biaxial stress</p>
---	--	--	--

<p>Aeronautical Systems Division, AF Materials Laboratory, Metals and Ceramics Division, Wright-Patterson AFB, Ohio.</p> <p>Rept No. ASD-TDR-63-647. MATERIAL DAMPING UNDER BIAXIAL STATE OF STRESS GENERATED BY COMBINED AXIAL AND INTERNAL PRESSURE LOADINGS. Final report, July 63, 30pp. Incl illus., tables, & refs.</p> <p>Unclassified Report</p> <p>A test machine has been constructed which measures material damping in thin-walled, cylindrical specimens subject to combined internal pressure and axial cyclic loading. The purpose of this machine is to allow the complete range of biaxial stress states to be developed, so that the individual damping effects of distortional and dilatational</p> <p>(over)</p>	<p>1. Material damping</p> <p>2. Mechanical properties</p> <p>3. Biaxial stress</p> <p>4. Biaxial stress damping apparatus</p> <p>I. AFSC Project 7351, Task 735106</p> <p>II. Contract No. AF 33(657)-7453</p> <p>III. University of Minnesota, Minneapolis, Minn.</p> <p>IV. F. J. Mentel</p> <p>S. H. Chi</p> <p>V. Avail for OPS</p> <p>VI. In ASTIA collection</p>	<p>1. Material damping</p> <p>2. Mechanical properties</p> <p>3. Biaxial stress</p> <p>4. Biaxial stress damping apparatus</p> <p>I. AFSC Project 7351, Task 735106</p> <p>II. Contract No. AF 33(657)-7453</p> <p>III. University of Minnesota, Minneapolis, Minn.</p> <p>IV. F. J. Mentel</p> <p>S. H. Chi</p> <p>V. Avail for OPS</p> <p>VI. In ASTIA collection</p>	<p>1. Material damping</p> <p>2. Mechanical properties</p> <p>3. Biaxial stress</p> <p>4. Biaxial stress damping apparatus</p> <p>I. AFSC Project 7351, Task 735106</p> <p>II. Contract No. AF 33(657)-7453</p> <p>III. University of Minnesota, Minneapolis, Minn.</p> <p>IV. F. J. Mentel</p> <p>S. H. Chi</p> <p>V. Avail for OPS</p> <p>VI. In ASTIA collection</p>
<p>strain rate might be clearly discerned. Experimental results on a series of magnesium alloy specimens are found to display significant damping effect associated with dilatational straining.</p> <p>ASD-TDR-63-647</p>	<p>strain rate might be clearly discerned. Experimental results on a series of magnesium alloy specimens are found to display significant damping effect associated with dilatational straining.</p> <p>ASD-TDR-63-647</p>	<p>strain rate might be clearly discerned. Experimental results on a series of magnesium alloy specimens are found to display significant damping effect associated with dilatational straining.</p> <p>ASD-TDR-63-647</p>	<p>strain rate might be clearly discerned. Experimental results on a series of magnesium alloy specimens are found to display significant damping effect associated with dilatational straining.</p> <p>ASD-TDR-63-647</p>

<p>Aeronautical Systems Division, AF Materials Laboratory, Metals and Ceramics Division, Wright-Patterson AFB, Ohio.</p> <p>Rept No. ASD-TR-63-647. MATERIAL DAMPING UNDER BIAXIAL STRESS OF STRESS ORIGINATED BY COMBINED AXIAL AND INTERNAL PRESSURE LOADINGS. Final report, July 63, 30pp. Incl illus., tables, & refs.</p> <p>Unclassified Report</p> <p>A test machine has been constructed which measures material damping in thin-walled, cylindrical specimens subject to combined internal pressure and axial cyclic loading. The purpose of this machine is to allow the complete range of biaxial stress states to be developed, so that the individual damping effects of distortional and dilatational</p> <p>(over)</p>	<ol style="list-style-type: none"> 1. Material damping 2. Mechanical properties 3. Biaxial stress 4. Biaxial stress damping apparatus <ol style="list-style-type: none"> I. AFSC Project 7751, Task 735106 II. Contract No. AF 33(657)-7453 III. University of Minnesota, Minneapolis, Minn. IV. T. J. Mottel V. S. H. Chi V. Anal Cr OTR VI. In ASTIA collection 	<p>Aeronautical Systems Division, AF Materials Laboratory, Metals and Ceramics Division, Wright-Patterson AFB, Ohio.</p> <p>Rept No. ASD-TR-63-647. MATERIAL DAMPING UNDER BIAXIAL STRESS OF STRESS ORIGINATED BY COMBINED AXIAL AND INTERNAL PRESSURE LOADINGS. Final report, July 63, 30pp. Incl illus., tables, & refs.</p> <p>Unclassified Report</p> <p>A test machine has been constructed which measures material damping in thin-walled, cylindrical specimens subject to combined internal pressure and axial cyclic loading. The purpose of this machine is to allow the complete range of biaxial stress states to be developed, so that the individual damping effects of distortional and dilatational</p> <p>(over)</p>	<ol style="list-style-type: none"> 1. Material damping 2. Mechanical properties 3. Biaxial stress 4. Biaxial stress damping apparatus <ol style="list-style-type: none"> I. AFSC Project 7751, Task 735106 II. Contract No. AF 33(657)-7453 III. University of Minnesota, Minneapolis, Minn. IV. T. J. Mottel V. S. H. Chi V. Anal Cr OTR VI. In ASTIA collection
<p>straining action might be clearly discerned. Experimental results on a series of unannealed alloy specimens are found to display significant damping effect associated with dilatational straining.</p> <p>AD-675-647-10</p>		<p>straining action might be clearly discerned. Experimental results on a series of unannealed alloy specimens are found to display significant damping effect associated with dilatational straining.</p> <p>AD-675-647-10</p>	

<p>Aeronautical Systems Division, AF Materials Laboratory, Metals and Ceramics Division, Wright-Patterson AFB, Ohio.</p> <p>Rpt No. ASD-TIR-63-647. MATERIAL DAMPING UNDER BIAXIAL STATE OF STRESS GENERATED BY COMBINED AXIAL AND INTERNAL PRESSURE LOADINGS. Final report, July 63, 30pp. Incl illus., tables, & refs..</p> <p>Unclassified Report</p> <p>A test machine has been constructed which measures material damping in thin-walled, cylindrical specimens subject to combined internal pressure and axial cyclic loading. The purpose of this machine is to allow the complete range of biaxial stress states to be developed, so that the individual damping effects of distortional and dilatational</p> <p>(over)</p>	<ol style="list-style-type: none"> 1. Material damping 2. Mechanical properties 3. Biaxial stress 4. Biaxial stress damping apparatus I. AFSC Project 7351, Task 735106 II. Contract No. AP 33(637)-7453 III. University of Minnesota, Minneapolis, Minn. IV. T. J. Mentel S. H. Chi V. Avail fr OTS VI. In ASTIA collection 	<p>Aeronautical Systems Division, AF Materials Laboratory, Metals and Ceramics Division, Wright-Patterson AFB, Ohio.</p> <p>Rpt No. ASD-TIR-63-647. MATERIAL DAMPING UNDER BIAXIAL STATE OF STRESS GENERATED BY COMBINED AXIAL AND INTERNAL PRESSURE LOADINGS. Final report, July 63, 30pp. Incl illus., tables, & refs..</p> <p>Unclassified Report</p> <p>A test machine has been constructed which measures material damping in thin-walled, cylindrical specimens subject to combined internal pressure and axial cyclic loading. The purpose of this machine is to allow the complete range of biaxial stress states to be developed, so that the individual damping effects of distortional and dilatational</p> <p>(over)</p>	<ol style="list-style-type: none"> 1. Material damping 2. Mechanical properties 3. Biaxial stress 4. Biaxial stress damping apparatus I. AFSC Project 7351, Task 735106 II. Contract No. AP 33(637)-7453 III. University of Minnesota, Minneapolis, Minn. IV. T. J. Mentel S. H. Chi V. Avail fr OTS VI. In ASTIA collection
<p>straining action might be clearly discerned. Experimental results on a series of magnesium alloy specimens are found to display significant damping effect associated with dilatational straining.</p>		<p>straining action might be clearly discerned. Experimental results on a series of magnesium alloy specimens are found to display significant damping effect associated with dilatational straining.</p>	